

See discussions, stats, and author profiles for this publication at: <https://www.researchgate.net/publication/23288097>

# Association Properties of $\beta$ B1- and $\beta$ A3-Crystallins: Ability To Form Heterotetramers †

ARTICLE *in* BIOCHEMISTRY · OCTOBER 2008

Impact Factor: 3.02 · DOI: 10.1021/bi8012438 · Source: PubMed

---

CITATIONS

18

---

READS

20

5 AUTHORS, INCLUDING:



May Chan

University of Michigan

20 PUBLICATIONS 89 CITATIONS

SEE PROFILE



Yuri Sergeev

U.S. Department of Health and Human Services

57 PUBLICATIONS 1,530 CITATIONS

SEE PROFILE

Published in final edited form as:

Biochemistry. 2008 October 21; 47(42): 11062–11069. doi:10.1021/bi8012438.

## Association Properties of $\beta$ B1- and $\beta$ A3-Crystallins: Ability to Form Heterotetramers

May P. Chan<sup>¶,1</sup>, Monika Dolinska<sup>¶</sup>, Yuri V. Sergeev<sup>¶</sup>, Paul T. Wingfield<sup>§</sup>, and J. Fielding Hejtmancik<sup>\*,¶</sup>

<sup>¶</sup>National Eye Institute, Bethesda, MD 20892

<sup>§</sup>National Institute of Arthritis and Musculoskeletal and Skin Diseases, National Institutes of Health, Bethesda, MD 20892

### Abstract

As major constituents of the mammalian lens,  $\beta$ -crystallins associate into dimers, tetramers, and higher-order complexes in order to maintain lens transparency and refractivity. A previous study has shown that dimerization of  $\beta$ B2- and  $\beta$ A3-crystallins is energetically highly favored and entropically driven. While heterodimers further associate into higher order complexes *in vivo*, a significant level of reversibly associated tetrameric crystallin has not been previously observed *in vitro*. In order to enhance our understanding of the interactions between  $\beta$ -crystallins, this study characterizes the association of  $\beta$ B1-crystallin, a major component of large  $\beta$ -crystallin complexes ( $\beta$ -high) with itself and with  $\beta$ A3-crystallin. Mouse  $\beta$ B1- and human  $\beta$ A3-crystallins were expressed in *E. coli* and purified chromatographically. Their association was then characterized using size-exclusion chromatography, native gel electrophoresis, isoelectric focusing, and analytical sedimentation equilibrium centrifugation. When present alone, each  $\beta$ -crystallin associates into homodimers but no tetramer formation is seen. Upon mixing, heterocomplex formation between  $\beta$ B1- and  $\beta$ A3-crystallins is observed using size-exclusion chromatography, native gel electrophoresis, isoelectric focusing, and sedimentation equilibrium. In contrast to results previously obtained upon mixing  $\beta$ B2- and  $\beta$ A3-crystallins, mixed  $\beta$ B1- and  $\beta$ A3-crystallins show a dimer-tetramer equilibrium with a  $K_d$  of 1.1  $\mu$ M, indicating that these two  $\beta$ -crystallins associate predominantly into heterotetramers *in vitro*. Thus, while each purified  $\beta$ -crystallin associates only into homodimers and mixed  $\beta$ B2- and  $\beta$ A3-crystallins form a mixture of homo- and heterodimers, mixed  $\beta$ B1- and  $\beta$ A3-crystallins associate predominantly into heterotetramers in equilibrium with heterodimers. These findings suggest a unique role for  $\beta$ B1-crystallin in promoting higher-order crystallin association in the lens.

Crystallins, which exist at extremely high concentrations in the eye lens, are structural proteins critical for transmitting and focusing light. The human lens contains  $\alpha$ -,  $\beta$ -, and  $\gamma$ -crystallins, of which  $\beta$ -crystallins, taken as a whole, represent the greatest part. Seven different subtypes of  $\beta$ -crystallins have been identified in the human lens, four of which are relatively acidic ( $\beta$ A1,  $\beta$ A2,  $\beta$ A3, and  $\beta$ A4), and three of which are relatively basic ( $\beta$ B1,  $\beta$ B2, and  $\beta$ B3).  $\beta$ - and  $\gamma$ -crystallins, which have highly similar core sequences, form the  $\beta\gamma$ -crystallin superfamily. Structurally, both  $\beta$ - and  $\gamma$ -crystallins contain two homologous domains connected by a short connecting sequence. Each domain contains two Greek-key motifs, and each motif comprises four antiparallel  $\beta$ -sheets (1).  $\beta$ -Crystallins contain N-terminal extensions ranging in length from 12 to 57 amino acids. In addition, the basic  $\beta$ -crystallins contain C-terminal extensions ranging from 11 to 16 amino acids.  $\beta$ -Crystallins are highly conserved across species with

\*Address correspondence to: J. Fielding Hejtmancik, OGVFB/NEI/NIH, 10/10B10, 10 Center Drive, Bethesda, MD 20892; Tel. 301-496-8300; fax: 301-435-1598; Email: f3h@nei.nih.gov.

<sup>1</sup>Supported by the Howard Hughes Medical Institute Research Scholars Program.

$\beta$ A3-crystallin being over 95% identical between mouse and human. In contrast to  $\beta$ -crystallins,  $\beta$ -crystallins have either no terminal extensions or short extensions containing only a few amino acids (2).

$\beta$ -Crystallins are known to associate into dimers, tetramers, and higher-order complexes *in vivo*. Size-exclusion chromatography of bovine or human lens extracts shows three size classes of  $\beta$ -crystallin complexes:  $\beta$ H (160-200 kDa, primarily octamers),  $\beta$ L1 (70-100 kDa, primarily tetramers), and  $\beta$ L2 (46-50 kDa, primarily dimers) (3;4). The distribution of  $\beta$ -crystallins among different size classes is dependent on protein concentration, pH, and ionic strength (5; 6). Despite the sequence homology between  $\beta$ - and  $\gamma$ -crystallins,  $\gamma$ -crystallins are observed in the lens strictly as monomers, which have prompted investigations into the role of terminal extensions in crystallin association. Previous studies have shown that although the terminal arms of  $\beta$ -crystallins are not required for association, the N-terminal extension of  $\beta$ A3-crystallin assists in self-association into homodimers, while the N-terminal extension of  $\beta$ B2-crystallin actually decreases association into homodimers (7;8). Several studies have also demonstrated a correlation between the length of the N-terminal extension of  $\beta$ B1-crystallin in lens extracts and the size class in which it migrates on size exclusion chromatography (9-11). Bateman et al. have previously shown that a truncated form of  $\beta$ B1- and  $\beta$ A3-crystallin migrate at a size of approximately 100 kDa on gel permeation chromatography, and have a similar size as estimated by laser light scattering.(12)

While  $\beta$ -crystallins are known to form oligomers *in vivo*, a significant level of tetramers or higher-order complexes generally has not been observed in previous *in vitro* studies. This can be explained in part by the lower protein concentration being examined *in vitro*, compared with the extremely high concentration in the eye lens. It has previously been demonstrated that both mouse  $\beta$ B2-crystallin and human  $\beta$ A3-crystallin form reversible homodimers when present alone, and that these readily form heterodimers upon mixing and incubation at room temperature in the absence of denaturants (13). However, no heterotetramers or higher-order complexes were observed between these two crystallins. The current study employs a similar strategy to study the association properties of another pair of  $\beta$ -crystallins—mouse  $\beta$ B1- and human  $\beta$ A3-crystallins. When present alone, each protein associates into homodimers but neither forms homotetramers. Upon mixing in the absence of denaturants, heterocomplex formation between these two  $\beta$ -crystallin subtypes was observed by size-exclusion chromatography, native gel electrophoresis, isoelectric focusing, and sedimentation equilibrium. In contrast to the previous results obtained with  $\beta$ B2- and  $\beta$ A3-crystallins, both size-exclusion chromatography and sedimentation equilibrium of the mixture of  $\beta$ B1- and  $\beta$ A3-crystallins show a dimer-tetramer equilibrium, with a  $K_d$  of 1.1  $\mu$ M calculated from the latter. These results show that mixed  $\beta$ B1- and  $\beta$ A3-crystallins associate predominantly into heterotetramers *in vitro*.

## EXPERIMENTAL PROCEDURES

### Expression and purification of $\beta$ B1-crystallin

Mouse cDNA encoding  $\beta$ B1-crystallin (consistent with NCBI sequence NM\_023695) was cloned into a pET-20b(+) vector (Novagen) utilizing the ATG codon of its Nde1 site (CATATG) as a start codon (generous gift of Dr. H. Mchaourab). The recombinant pET/ $\beta$ B1 plasmid was then used to transform competent BL21(DE3)pLysS cells according to the manufacturer's protocol (Invitrogen). Bacterial cultures were grown to an  $OD_{600}$  of 0.5-0.6, and induced for 2 hours with 1 mM IPTG. The harvested cell pellet was resuspended in Buffer A (50 mM Tris-HCl, 1 mM EDTA, 0.15 M NaCl, 1 mM DTT, 50  $\mu$ M TCEP, at pH 7.5) with added Complete Protease Inhibitors cocktail (Roche). Lysis was performed by sonication. The presence of  $\beta$ B1-crystallin was confirmed by SDS-PAGE. The lysate was centrifuged and the supernatant was dialyzed overnight against 2 liters of Buffer B (50 mM sodium phosphate, 1

mM EDTA, 1 mM DTT, and 50  $\mu$ M TCEP, at pH 6.8). The dialysate was then loaded on a HiTrap SP FF cation exchange chromatography column (GE Healthcare), and eluted with a gradient of 0 to 1 M NaCl in Buffer B. Fractions containing  $\beta$ 1-crystallin were pooled, concentrated, and chromatographed on a Superdex 75 HR16/60 size-exclusion chromatography column with Buffer A. The Superdex 75 column was precalibrated with the following low-molecular-weight standards: bovine serum albumin, ovalbumin, chymotrypsinogen, ribonuclease A, and acetone (Amersham Biosciences; Sigma-Aldrich). Fractions containing  $\beta$ 1-crystallin were pooled with a final purity of >95% as assessed by SDS-PAGE.

### Expression and purification of $\beta$ A3-crystallin

Human cDNA encoding  $\beta$ A3-crystallin (consistent with NCBI sequence NM\_005208) was cloned into pET-20b(+) utilizing the ATG codon of its NdeI restriction site as start codon. Recombinant pET/ $\beta$ A3 plasmid was then used to transform competent BL21(DE3) cells according to manufacturer's protocol (Invitrogen). Bacterial cultures were grown to an OD<sub>600</sub> of 0.5-0.6, and induced for 2 hours with 0.5 mM IPTG. The harvested cell pellet was resuspended in Buffer A. Lysis was performed by sonication. The presence of  $\beta$ A3-crystallin was confirmed by SDS-PAGE and Western blots using antibodies that target the first Greek-key motif of  $\beta$ A3-crystallin (a.a. 37-68: DQENFQGKRMEFTSSCPNVSENFNVRSLKV) (6). The lysate was centrifuged and the supernatant was dialyzed overnight against 2 L of Buffer C (50 mM Tris-HCl, 1 mM EDTA, 1 mM DTT, and 50  $\mu$ M TCEP, at pH 8.1). The dialysate was then loaded on a HiTrap DEAE FF anion exchange chromatography column (GE Healthcare), and eluted with a gradient of 0 to 1 M NaCl in Buffer C. Fractions containing  $\beta$ A3-crystallin were pooled, concentrated, and eluted on a Superdex 75 HR16/60 size-exclusion chromatography column with Buffer A. Fractions containing  $\beta$ A3-crystallin were pooled and showed a final purity of >95% as assessed by SDS-PAGE.

### Association of $\beta$ B1- and $\beta$ A3-crystallins

Purified  $\beta$ B1- and  $\beta$ A3-crystallins in Buffer A were adjusted to three sets of concentrations according to Table 1 (approximately 0.5, 1, and 2 mg/mL each), to give a 1:1 molar ratio when present in equal volumes. Concentrations were estimated from A<sub>280</sub> readings on a spectrophotometer. At each concentration, equal volumes of  $\beta$ B1- and  $\beta$ A3-crystallins were mixed and incubated at room temperature in Buffer C. Aliquots of 300  $\mu$ L and 30  $\mu$ L were taken at some or all of the following time points: 0, 0.5, 1, 2, 4, 6, 12, and 24 hours after mixing, and immediately frozen in ethanol-dry ice bath and stored at -80°C until ready for analyses.

### Chromatography and Electrophoresis

Each 300  $\mu$ L aliquot of the mixture of  $\beta$ B1- and  $\beta$ A3-crystallins was subsequently thawed and loaded on a Superdex 75 HR10/30 size-exclusion chromatography column (analytical grade) precalibrated with the same low-molecular-weight standards as mentioned before. Each sample was eluted with one bed volume (25 mL) of Buffer A and the A<sub>280</sub> was monitored throughout the run. For SDS-PAGE analysis, selected fractions were electrophoresed on ReadyGels (Tris-HCl, 4-15% gradient; BioRad) in Tris/glycine/SDS buffer at 200 V for 30 minutes, using a Benchmark Protein Ladder (Invitrogen) as molecular weight markers. For native gel electrophoresis, the 30  $\mu$ L aliquots were electrophoresed on ReadyGels in the same manner but in the absence of SDS.

### Analytical Ultracentrifugation

Prior to centrifugation, purified proteins were partially unfolded by adding 10 mM DTT and 1 M urea to the samples, incubated at room temperature for 30 minutes, and subsequently refolded by dialysis against 2 L of Buffer A without DTT at 4°C for 24 hours. Only samples

showing a single peak on size-exclusion chromatography and >95% purity on SDS-PAGE were used for analytical ultracentrifugation. Sample concentration was adjusted to 0.6 mg/mL. Centrifugation was done in a Beckman Optima XL-I analytical centrifuge. Absorption optics, an An-60 Ti rotor, and standard double-sector centerpiece cells were used. All analyses were performed using duplicate protein samples. Data were collected after 16 hours of centrifugation at 16,500 rpm at 20°C. The baselines were established by overspeeding at 45,000 rpm for another 4 hours. Equilibria profiles were analyzed by standard Optima XL-I Origin-based data analysis software. Solvent density was estimated as previously described (14).

Dissociation constants were determined by fitting either a monomer-dimer equilibrium curve (for  $\beta$ B1-crystallin) or a dimer-tetramer equilibrium curve (for  $\beta$ B1/ $\beta$ A3-heterocomplex) to the concentration gradient profile established at each temperature.

### Isoelectric focusing

Samples taken at various time points after mixing of  $\beta$ B1- and  $\beta$ A3-crystallins were electrofocused on nondenaturing PhastGels IEF 3-9 (Pharmacia). One  $\mu$ L of sample was applied in each lane. PhastSystem (Pharmacia) was set up to run the following protocol: (1) Prefocusing at 2000 V, 2.5 mA, 3.5 W, 15°C for 75 V·h; (2) Sample application at 200 V, 2.5 mA, 3.5 W, 15°C for 15 V·h; (3) Focusing at 2000 V, 2.5 mA, 3.5 W, 15°C for 410 V·h. Broad-range pI 3-10 markers (Pharmacia) were applied as standards. After isoelectric focusing, gels were fixed with 20% trichloroacetic acid, stained with 0.02% PhastGel Blue R solution (coomassie) in 30% methanol and 10% acetic acid with 0.1% (w/v)  $\text{CuSO}_4$ , and finally destained with 30% methanol and 10% acetic acid.

## RESULTS

### Expression of mouse $\beta$ B1-crystallin

Mouse  $\beta$ B1-crystallin is expressed as soluble protein with high yield in *E. coli*. Figure 1 shows the SDS-PAGE of the sample following purification by ion-exchange (A) and size-exclusion chromatography. A discrete band at 28 kDa is seen with a final purity of >95% (Figure 1B). This band reacts strongly with anti- $\beta$ H-crystallin antibodies on Western blot (data not shown). At 1 mg/mL,  $\beta$ B1-crystallin elutes on Superdex 75 column as a single peak with an apparent molecular weight of 37 kDa, intermediate between the predicted masses of monomeric (28 kDa) and dimeric (56 kDa)  $\beta$ B1-crystallin (Figure 2A). After incubation at room temperature for 24 hours,  $\beta$ B1-crystallin elutes again as a single peak, but at a slightly larger apparent size of 37.8 kDa (data not shown). This difference is small and of uncertain significance. The peaks are somewhat broad and slightly skewed, as is expected for a protein in rapid monomer-dimer equilibrium (7). Mass spectrometry shows the molecular mass to be 27,871.16 Da, consistent with the expected monomeric mass of 27,870 Da. The purified proteins were intact as assessed by SDS PAGE and no contaminating peptides were detected on mass spectrometry.

### Expression of human $\beta$ A3-crystallin

Human  $\beta$ A3-crystallin was expressed as soluble protein with high yield in *E. coli* as previously described (7). After purification by ion-exchange and size-exclusion chromatography as previously described (15), SDS-PAGE shows a discrete band at 25 kDa with a final purity of >95%. This band reacts strongly with anti- $\beta$ A3 antibodies on Western blots (data not shown). At 1 mg/mL,  $\beta$ A3-crystallin elutes on Superdex 75 column as a single peak with an apparent molecular weight of 41.3 kDa (Figure 2A). This is intermediate between the predicted masses of monomeric (25 kDa) and dimeric (50 kDa)  $\beta$ A3-crystallin. After incubation at room temperature for 24 hours,  $\beta$ A3-crystallin elutes as a single peak and shows minimal if any increase in its apparent molecular size (data not shown). The purified proteins were intact as assessed by SDS PAGE and no contaminating peptides were detected on mass spectrometry.

### Size-exclusion chromatography of mixed $\beta$ B1- and $\beta$ A3-crystallins

When  $\beta$ B1- and  $\beta$ A3-crystallins are mixed at 36  $\mu$ M (equivalent to approximately 1 mg/mL) each, allowed to stand at room temperature for varying periods of time, and chromatographed on a Superdex 75 column, one or two peaks are observed depending on the incubation time. These two distinct peaks have averaged apparent molecular masses of 71.1 kDa and 37.5 kDa, respectively (Figure 2B). At longer incubation times there is a clear trend towards an increasing amount of the higher-molecular-weight species (71.1 kDa), coupled with a decreasing amount of the lower-molecular-weight species (37.5 kDa) with an initial half life of about 5 hours. SDS-PAGE shows that at the beginning of the incubation (0 hour), the lower-molecular-weight peak comprises  $\beta$ B1- and  $\beta$ A3-crystallins that are asymmetrically distributed with  $\beta$ A3-crystallin appearing slightly before  $\beta$ B1-crystallin (Figure 2B-gel a). At the end of the incubation (24 hours), the higher-molecular-weight peak comprises samples with a 1:1 ratio of the two crystallins in the high molecular weight peak and some excess  $\beta$ B1-crystallin in smaller molecular weight fractions (Figure 2B-gel b, confirmed by scanning of the electrophoresed bands, data not shown).

When the initial concentration is doubled to 72  $\mu$ M (equivalent to approximately 2 mg/mL), a similar trend is observed, with both species showing slightly higher molecular masses (76.4 and 41.7 kDa, respectively) (Figure 2C). A similar trend is also observed when the initial concentration is lowered to 18  $\mu$ M (equivalent to approximately 0.5 mg/mL), but the peaks become less distinct as the levels approach the detection limit of the monitor (Figure 2D). A peak that corresponds to the higher-molecular-weight species has an averaged molecular weight of 69.6 kDa, which is slightly lower than that observed at higher concentrations, suggesting a rapid dimer-tetramer equilibrium for  $\beta$ B1-crystallin similar to that of  $\beta$ A3-crystallin monomers and dimers described in (7).

### Native gel electrophoresis of mixed $\beta$ B1- and $\beta$ A3-crystallins

Figure 3A shows native gel electrophoresis of  $\beta$ B1- and  $\beta$ A3-crystallin samples mixed at 1 mg/mL. The migration of  $\beta$ B1-crystallin is markedly retarded, with most of the protein retained at the loading position of the gels. Conversely,  $\beta$ A3-crystallin migrates well into the gels. Both concentrations display qualitatively similar patterns. No interaction between  $\beta$ B1- and  $\beta$ A3-crystallins is observed at time 0, followed by increasing formation of the intermediate species, and decreasing amounts of the starting proteins at successive time points. The most prominent intermediate band is located closer to the  $\beta$ B1-crystallin position than to the  $\beta$ A3-crystallin position (indicated by black arrow).

### Isoelectric focusing of mixed $\beta$ B1- and $\beta$ A3 crystallins

Figure 3B shows that  $\beta$ B1-crystallin electrofocuses at an isoelectric point slightly lower than 7.35, consistent with its predicted pI of 7.28.  $\beta$ A3-Crystallin electrofocuses slightly lower than pI 6.55, also consistent with its predicted pI of 6.20. Isoelectric focusing immediately after mixing essentially produces an overlay of the two patterns observed with the individual proteins. At increasing incubation times, less protein is observed at the pI's of the individual crystallins, while more protein is found at an intermediate pI, with two additional lighter and slightly more acidic bands also appearing as the incubation progresses. Formation of the intermediate species becomes noticeable by 0.5 hour after mixing, and appears to be approaching equilibrium at 12 hours, at which point most protein is present as the intermediate species.

### Sedimentation equilibrium of $\beta$ B1-crystallin

Sedimentation equilibrium analysis of purified mouse  $\beta$ B1-crystallin shows that the experimental values fit closely with the predicted monomer-dimer model at 20°C (Figure 4A).



Assuming a monomer-dimer equilibrium, the dissociation constant ( $K_d$ ) is  $1.55 \pm 0.20 \mu\text{M}$  and weight-average molecular weight ( $M_r$ ) is determined to be  $47,295 \pm 276 \text{ Da}$ . Comparison of the average  $K_d$  and  $M_r$  of mouse  $\beta\text{B1-}$ ,  $\beta\text{A3-}$ , and  $\beta\text{B2-crystallins}$  is shown in Table 2.

### Sedimentation equilibrium of $\beta\text{B1}/\beta\text{A3}$ heterotetramer

Figure 4B shows that at  $20^\circ\text{C}$ ,  $\beta\text{B1-}$  and  $\beta\text{A3-crystallins}$  form heterocomplexes that fit well with the predicted dimer-heterotetramer equilibrium, with a  $K_d$  of  $1.1 \mu\text{M}$ . The average molecular weight of the complex is determined to be  $95,998 \pm 714.9 \text{ Da}$  at  $20^\circ\text{C}$ , which is close to the predicted mass of the heterotetramer containing two subunits of each crystallin ( $106.2 \text{ kDa}$ ).

## DISCUSSION

Here we describe the association of mouse  $\beta\text{B1-}$  and human  $\beta\text{A3-crystallins}$ . When present alone, each protein associates into homodimers but neither forms homotetramers, similar to results obtained with  $\beta\text{B2-}$  and  $\beta\text{A3-crystallins}$ . However, in contrast to the previous results obtained from  $\beta\text{B2-}$  and  $\beta\text{A3-crystallins}$ , mixed  $\beta\text{B1-}$  and  $\beta\text{A3-crystallins}$  show a dimer-tetramer equilibrium, with a  $K_d$  of  $1.1 \mu\text{M}$ . Thus mixed  $\beta\text{B1-}$  and  $\beta\text{A3-crystallins}$  associate predominantly into heterotetramers *in vitro*.

Mouse  $\beta\text{B1-crystallin}$  was faithfully expressed with high yield in BL21(DE3)pLysS, which is the same system used previously for expressing human  $\beta\text{B1-crystallin}$  by Lampi *et al.* (16). The identity of the expressed  $\beta\text{B1-crystallin}$  is supported by its correct molecular mass on SDS-PAGE and mass spectrometry. Human  $\beta\text{A3-crystallin}$  was previously expressed using the baculovirus system (6). This study utilized the bacterial system BL21(DE3), which is a more convenient and equally productive method for the expression of relatively stable proteins, such as human  $\beta\text{A3-crystallin}$ . The identity of the expressed  $\beta\text{A3-crystallin}$  is confirmed by its molecular mass on SDS-PAGE and its strong reactivity with antibodies that specifically target the first Greek-key motif of bovine  $\beta\text{A3-crystallin}$  (data not shown). While mouse and human  $\beta\text{B1-crystallins}$  are only 80.9% identical (90% similar), mouse and human  $\beta\text{A3-crystallins}$  share a 95.3% identity (100% similarity), suggesting that the use of human and mouse crystallins provides a reasonably accurate model of crystallin behavior, especially in the mouse lens. Also, while the conserved PAPA sequence is more evident in mouse  $\beta\text{B1-crystallin}$ , human  $\beta\text{B1-crystallin}$  is predicted to share similar structural characteristics in this region by both Chou-Fasman and Garnier-Robson algorithms (data not shown).

Size-exclusion chromatography of mouse  $\beta\text{B1-crystallin}$  at  $1 \text{ mg/mL}$  shows a somewhat broad and asymmetrical single peak with an apparent molecular weight that is intermediate between the monomeric and dimeric forms, consistent with a monomer-dimer equilibrium (17). An intermediate molecular weight is observed as monomers constantly associate and dissociate in a rapidly reversible manner as the protein is chromatographed (17). The homodimer formation observed in this study agrees with other reports of  $\beta\text{B1-crystallin}$  (16;18) and most other  $\beta\text{-crystallins}$ , including  $\beta\text{A3-}$  and  $\text{B2-crystallins}$  (6;13). However, while size exclusion chromatography in these studies has suggested that  $\beta\text{B1-crystallin}$  might behave as a dimer as concentrations increase above  $10 \text{ mg/ml}$  (18) or at  $0.7 \text{ mg/ml}$  (16), light scattering suggests molecular masses consistent with a dimer with a small population in aggregates of  $264 \text{ kDa}$  (16) or varying between  $48 \text{ kDa}$  and  $125 \text{ kDa}$  depending on the protein concentration (18). While the nature of the higher aggregates is unclear from the data presented, they do not appear to represent the reversible high affinity association described here. Rather, the data suggest either a stable high molecular weight complex co-existing with a lower dimeric form in some cases and a gradual smooth increase in molecular mass in others.

The stability of  $\beta$ B1-crystallin over time is supported by its molecular weight, which remains relatively constant after 24 hours of incubation at room temperature. Similar results were obtained for  $\beta$ A3-crystallin, which also displays persistent monomer-dimer equilibrium. Despite having a smaller predicted molecular size,  $\beta$ A3-crystallin shows a higher apparent molecular weight on size exclusion chromatography than  $\beta$ B1-crystallin. Delayed elution of  $\beta$ B1-crystallin from size exclusion chromatography has been reported previously(16;18) and has been attributed to interaction between  $\beta$ B1-crystallin and the column matrix, as is seen with amino-truncated  $\beta$ A3-crystallin,(8) . However, it is also consistent with the higher affinity for self-dimerization of  $\beta$ A3-crystallin relative to  $\beta$ B1-crystallin. The increase of the apparent molecular weight with increasing  $\beta$ B1-crystallin concentration on size exclusion chromatography suggests that the delayed elution of  $\beta$ B1-crystallin is due to reversible monomer-dimer equilibrium rather than interactions with the column or unusual effects of an unusual shape of the molecule, or perhaps both might contribute to some degree.

Sedimentation equilibrium of mouse  $\beta$ B1-crystallin at 0.6 mg/mL and 20°C again confirms a monomer-dimer equilibrium. In contradistinction to some previous reports,(18) no evidence for homotetramer formation was seen with analytical ultracentrifugation or size exclusion chromatography in these studies. The apparent average molecular weight estimated from sedimentation equilibrium at 20°C (47 kDa) is significantly higher than that estimated from size-exclusion chromatography (37 kDa). This discrepancy may be attributed to the fact that the association of crystallins is dependent on protein concentration, but also might reflect a tendency of  $\beta$ B1-crystallin to stick to the gel matrix in a size-exclusion column as discussed above. While the sedimentation study does not involve any elution buffer, size-exclusion chromatography subjects protein samples to dilution by the running buffer. As protein concentration drops, the monomer-dimer equilibrium is expected to shift towards monomer, thus resulting in a lower apparent molecular weight.

When mouse  $\beta$ B1-crystallin and human  $\beta$ A3-crystallin are incubated together at room temperature, heterocomplex formation is readily appreciable within 30 minutes by size-exclusion chromatography, native gel electrophoresis, and isoelectric focusing. In Figure 2, the higher-molecular-weight species that increases in amount with incubation time represents a dimer-tetramer equilibrium, as it corresponds to an apparent molecular weight that is intermediate between that of a dimer (either homodimer or heterodimer) and that of a tetramer. A number of observations suggest that this peak represents tetramer rather than trimer formation. As is seen with  $\beta$ A3- and  $\beta$ B1-crystallins in isolation, the apparent molecular weight increases towards the predicted tetramer size with increasing protein concentration.

SDS-PAGE of the eluted fractions shows that this peak contains equal amounts of  $\beta$ B1- and  $\beta$ A3-crystallins (Figure 2B). This 1:1 ratio suggests that each tetramer is composed on average of two subunits of  $\beta$ B1-crystallin and two subunits of  $\beta$ A3-crystallin. Conversely, the lower-molecular-weight species corresponds to a monomer-dimer equilibrium that decreases in amount over time. SDS-PAGE of this peak shows an asymmetric distribution of  $\beta$ B1- and  $\beta$ A3-crystallins, suggesting lack of interaction at the beginning of the incubation, and perhaps a tendency of  $\beta$ B1-crystallin to stick to the column matrix. In theory, three types of dimers can be present:  $\beta$ B1-homodimers (56 kDa),  $\beta$ A3-homodimers (50 kDa), and  $\beta$ B1/ $\beta$ A3-heterodimers (53 kDa). It is likely that the proximity in molecular masses of these three species has exceeded the resolution capacity of the Superdex 75 column, resulting in a broad single peak. While the exact mechanism of heterotetramer formation is unknown, it seems likely that it is via the association of two  $\beta$ B1/ $\beta$ A3-heterodimers rather than association of a  $\beta$ B1-homodimer with a  $\beta$ A3-homodimer. Ultimately, one would expect the mixture to reach a steady state of heterodimer-heterotetramer equilibrium. These data are in agreement with those of Bateman et al.(12). As expected, the final amount of heterotetramer formed is dependent on crystallin concentration. As protein concentration increases, the percentage of protein at the



molecular masses representing both monomer-dimer and dimer-tetramer equilibria increase, and vice versa (Figures 2B-2D). This indicates that higher concentrations shift the equilibria towards association.

Native gel electrophoresis, which separates proteins in their native states, provides additional information on the shapes of the complexes. Of interest, the migration of  $\beta$ B1-crystallin by itself is markedly retarded with some protein not entering the gel (Figure 3A). One possible explanation is that the N-terminal extension of  $\beta$ B1-crystallin, being the longest among all  $\beta$ -crystallins, severely hinders the migration of monomeric/dimeric  $\beta$ B1-crystallin through the polyacrylamide gel matrix. The intermediates formed over time, representing heterocomplex formation with  $\beta$ A3-crystallin, migrate further down the gel compared to  $\beta$ B1-crystallin alone. This suggests the interaction between  $\beta$ B1- and  $\beta$ A3-crystallins gives rise to a conformation that is more compact and thus penetrates the matrix more easily. One possibility is that the N-terminal arm of  $\beta$ B1-crystallin may be involved in holding the heterocomplex in place and thus becomes less flexible in the tetramer (19), protruding less and allowing migration of the complex into the gel. Alternatively, the  $\beta$ B1-crystallin N-terminal arm might interact with the gel matrix less in heterotetramers, which would also allow the heterocomplex to migrate further than the  $\beta$ B1-crystallin dimer.

Heterocomplex formation is also confirmed by isoelectric focusing. As expected, the heterocomplex has a pI that is intermediate between that of  $\beta$ B1-crystallin and of  $\beta$ A3-crystallin (Figure 3B). While this technique does not distinguish between heterodimer and heterotetramer formation, the absence of homodimers or homotetramers, which would have identical isoelectric points, after longer incubation times suggests that most of the intermediate band is composed of heterotetramers. This can be seen in comparison to isoelectric focusing of mixed  $\beta$ B2- and  $\beta$ A3-crystallins, in which the heterodimer and two homodimers coexist in a 2-1-1 ratio (13). That is, at equilibrium there is twice as much heterodimer as there is of each homodimer, suggesting that none of the three possible dimers is energetically favored over the other.

Finally, analytical ultracentrifugation provides thermodynamic characterization of the heterocomplex equilibrium. The experimental data fit well with the expected gradient of the heterodimer-heterotetramer equilibrium, with a  $K_d$  of 1.1  $\mu$ M. The observed molecular weight (96 kDa) is consistent with the predicted molecular weight of the heterotetramer consisting of two  $\beta$ B1- and two  $\beta$ A3-crystallin subunits (106.2 kDa), but significantly higher than the apparent molecular weight estimated from size-exclusion chromatography (69.6-76.4 kDa). Again, this may be due to the dilution effect during chromatography or adherence of the  $\beta$ B1-crystallin protein to the size exclusion chromatography gel matrix or both.

The formation of heterotetramers by mixed  $\beta$ B1- and  $\beta$ A3-crystallin contrasts with the lack of tetramers seen under similar conditions with mixed  $\beta$ B2- and  $\beta$ A3-crystallin (7;8). However, this is consistent with the high  $\beta$ B1-crystallin content observed in  $\beta$ H aggregates synthesized *in vivo* (5;20).  $\beta$ B2-crystallin, on the other hand, is present in all size-classes and is the primary constituent of  $\beta$ L2-crystallin (20), suggesting  $\beta$ B2-crystallin might have a low affinity for higher-order association with other  $\beta$ -crystallins. These observations might relate to the structural difference between  $\beta$ B2- and  $\beta$ B1-crystallins. The major factor that distinguishes  $\beta$ B1-crystallin from other  $\beta$ -crystallins, and especially basic  $\beta$ -crystallins, is its extremely long N-terminal extension containing 57 residues including a PAPA sequence (21). We hypothesize that  $\beta$ B1-crystallin may promote higher-order complex formation with other  $\beta$ -crystallins in the lens through the action of its long N-terminal extension. While it cannot, by itself, account for the formation of  $\beta$ H-crystallin oligomers, this does agree with the presence of  $\beta$ B1-crystallin preferentially in the  $\beta$ H complexes and truncated  $\beta$ B1-crystallins in  $\beta$ L1 and  $\beta$ L2 complexes previously described (9).

It is important to realize that under physiologic conditions, where protein concentration exceeds 300 mg/mL, higher-order association between  $\beta$ -crystallins would be favored. Therefore,  $\beta$ B1-crystallin might have a crucial role in associating with other  $\beta$ -crystallins in higher order complexes. We have not been able to measure the dissociation constant of the putative  $\beta$ B1  $\beta$ A3-crystallin heterodimer. However, if it has a similar dissociation constant to the  $\beta$ B1 homodimer the fraction of heterotetramer at 300 mg/ml would be greater than 99.99%, and this fraction would still approach 99.9% at 1 mg/ml. Thus, as has been previously suggested, the rapid interchange of crystallins might have more physiological implications than the existence of monomer or even dimer forms of the protein. This being said, the findings in this study have implications in cataractogenesis of the aging lens where N-terminal truncation of  $\beta$ B1-crystallin has been well documented (10;22). In this regard, the size distribution of  $\beta$ -crystallins is dependent on the age of the lens, which is itself correlated with crystallin modifications including truncation of the terminal arms (10;11). Finally, the lack of homotetramer formation *in vitro* indicates that higher-order association between different  $\beta$ -crystallin subtypes is favored over self-association. This supports a previous suggestion that acidic  $\beta$ -crystallins may preferentially associate with basic  $\beta$ -crystallins (23), although this may well result from heterotetramer/ heterodimer equilibrium with  $\beta$ B1- and  $\beta$ A3-crystallins as opposed to the heterodimer in which  $\beta$ B2- and  $\beta$ A3-crystallins associate into  $\beta$ B2 homodimers: $\beta$ B2- $\beta$ A3 heterodimers: $\beta$ A3 homodimers with a roughly 1:2:1 ratio (13;15).

In summary, this study has demonstrated for the first time reversible spontaneous *in vitro* formation of heterotetramers by  $\beta$ -crystallins. When present alone under these conditions,  $\beta$ B1- and  $\beta$ A3-crystallin associate into homodimers but neither forms homotetramers. Upon mixing under physiological conditions, heterocomplex formation between these two  $\beta$ -crystallin subtypes was observed by size-exclusion chromatography, native gel electrophoresis, isoelectric focusing, and sedimentation equilibrium. In contrast to the previous results obtained from  $\beta$ B2- and  $\beta$ A3-crystallins, which did not show tetramer formation, analytical centrifugation shows a dimer-tetramer equilibrium with a  $K_d$  of 1.1  $\mu$ M, suggesting that  $\beta$ B1- and  $\beta$ A3-crystallins associate predominantly into heterotetramers *in vitro*. Although we suspect that heterotetramers are formed preferentially through the interaction of two heterodimers ( $\beta$ B1/ $\beta$ A3 +  $\beta$ B1/ $\beta$ A3) these studies are unable to discriminate this mechanism from that involving the interaction between two homodimers ( $\beta$ B1/ $\beta$ B1 +  $\beta$ A3/ $\beta$ A3) or mixtures of both hetero- and homodimers. Future studies will address this question, as well as elucidating the molecular mechanisms of  $\beta$ B1-crystallin association into both dimers and heterotetramers.

## References

1. Wistow G, Turnell B, Summers L, Slingsby C, Moss D, Miller L, Lindley P, Blundell T. X-ray analysis of the eye lens protein gamma-II crystallin at 1.9 Å resolution. *J. Mol. Biol* 1983;170:175–202. [PubMed: 6631960]
2. Hejtmancik, JF.; Piatigorsky, J. Lens Proteins and their Molecular Biology. In: Alpert, DM.; Jakobiec, FA.; Azar, DT.; Gragoudas, ES., editors. *Principles and Practice of Ophthalmology*. W.B.Saunders Co.; Philadelphia: 2000. p. 1409-1428.
3. Bindels JG, Koppers A, Hoenders HJ. Structural aspects of bovine beta-crystallins: physical characterization including dissociation-association behavior. *Exp. Eye Res* 1981;33:333–343. [PubMed: 7286088]
4. Zigler JS Jr, Horwitz J, Kinoshita JH. Human beta-crystallin. I. Comparative studies on the beta 1, beta 2 and beta 3-crystallins. *Exp. Eye Res* 1980;31:41–55. [PubMed: 6775970]
5. Siezen RJ, Anello RD, Thompson JD. Interactions of Lens Proteins. Concentration dependence of beta-crystallin aggregation. *Exp. Eye Res* 1986;43:293–303. [PubMed: 3780875]
6. Hope JN, Chen HC, Hejtmancik JF. BetaA3/A1-crystallin association: role of the amino terminal arm. *Protein. Eng* 1994;7:445–451. [PubMed: 8177894]

7. Sergeev YV, Wingfield PT, Hejtmancik JF. Monomer-dimer equilibrium of normal and modified beta A3-crystallins: experimental determination and molecular modeling. *Biochemistry* 2000;39:15799–15806. [PubMed: 11123905]
8. Sergeev YV, Hejtmancik JF, Wingfield PT. Energetics of Domain-Domain Interactions and Entropy Driven Association of beta-Crystallins. *Biochemistry* 2004;43:415–424. [PubMed: 14717595]
9. Ajaz MS, Ma Z, Smith DL, Smith JB. Size of human lens beta-crystallin aggregates are distinguished by N-terminal truncation of betaB1. *J. Biol. Chem* 1997;272:11250–11255. [PubMed: 9111027]
10. Lampi KJ, Ma Z, Hanson SR, Azuma M, Shih M, Shearer TR, Smith DL, Smith JB, David LL. Age-related changes in human lens crystallins identified by two-dimensional electrophoresis and mass spectrometry. *Exp. Eye Res* 1998;67:31–43. [PubMed: 9702176]
11. Ma Z, Hanson SR, Lampi KJ, David LL, Smith DL, Smith JB. Age-related changes in human lens crystallins identified by HPLC and mass spectrometry. *Exp. Eye Res* 1998;67:21–30. [PubMed: 9702175]
12. Bateman OA, Sarra R, Van Genesen ST, Kappe G, Lubsen NH, Slingsby C. The stability of human acidic beta-crystallin oligomers and hetero-oligomers. *Exp. Eye Res* 2003;77:409–422. [PubMed: 12957141]
13. Hejtmancik JF, Wingfield P, Chambers C, Russell P, Chen H-C, Sergeev YV, Hope JN. Association properties of beta-B2- and betaA3-crystallin: ability to form dimers. *Protein. Eng* 1997;10:1347–1352. [PubMed: 9514125]
14. Laue, TM.; Shah, BD.; Ridgeway, TM.; Pelletier, SL. Computer-aided interpretation of analytical sedimentation data for proteins. In: Harding, SE.; Rowe, AJ.; Horton, JC., editors. *Analytical Ultracentrifugation in Biochemistry and Polymer Science*. Royal Society for Chemistry; Cambridge, United Kingdom: 1992. p. 90-125.
15. Hope JN, Chen H-C, Hejtmancik JF. Aggregation of betaA3-crystallin is independent of the specific sequence of the domain connecting peptide. *J. Biol. Chem* 1994;269:21141–21145. [PubMed: 8063735]
16. Lampi KJ, Oxford JT, Bachinger HP, Shearer TR, David LL, Kapfer DM. Deamidation of human beta B1 alters the elongated structure of the dimer. *Exp. Eye Res* 2001;72:279–288. [PubMed: 11180977]
17. Winzor DJ, Scheraga HA. Studies of chemically reacting systems on sephadex: chromatographic demonstration of the Gilbert Theory. *Biochemistry* 1963;2:1263–1267. [PubMed: 14093900]
18. Bateman OA, Lubsen NH, Slingsby C. Association behaviour of human betaB1-crystallin and its truncated forms. *Exp. Eye Res* 2001;73:321–331. [PubMed: 11520107]
19. Lapatto R, Nalini V, Bax B, Driessen H, Lindley PF, Blundell TL, Slingsby C. High resolution structure of an oligomeric eye lens beta-crystallin: loops, arches, linkers and interfaces in betaB2 dimer compared to a monomeric gamma-crystallin. *J. Mol. Biol* 1991;222:1067–1083. [PubMed: 1762146]
20. Slingsby C, Bateman OA. Rapid separation of bovine beta-crystallin subunits beta B1, beta B2, beta B3, beta A3 and beta A4. *Exp. Eye Res* 1990;51:21–26. [PubMed: 2373177]
21. Hejtmancik JF, Thompson MA, Wistow G, Piatigorsky J. cDNA and deduced protein sequence for the beta B1-crystallin polypeptide of the chicken lens: Conservation of the PAPA sequence. *J. Biol. Chem* 1986;261:982–987. [PubMed: 3753603]
22. David LL, Lampi KJ, Lund AL, Smith JB. The sequence of human betaB1-crystallin cDNA allows mass spectrometric detection of betaB1 protein missing portions of its N-terminal extension. *J. Biol. Chem* 1996;271:4273–4279. [PubMed: 8626774]
23. Slingsby C, Bateman OA. Quarternary interactions in eye lens beta-crystallins: basic and acidic subunits of beta-crystallins favor heterologous association. *Biochemistry* 1990;29:6592–6599. [PubMed: 2397202]

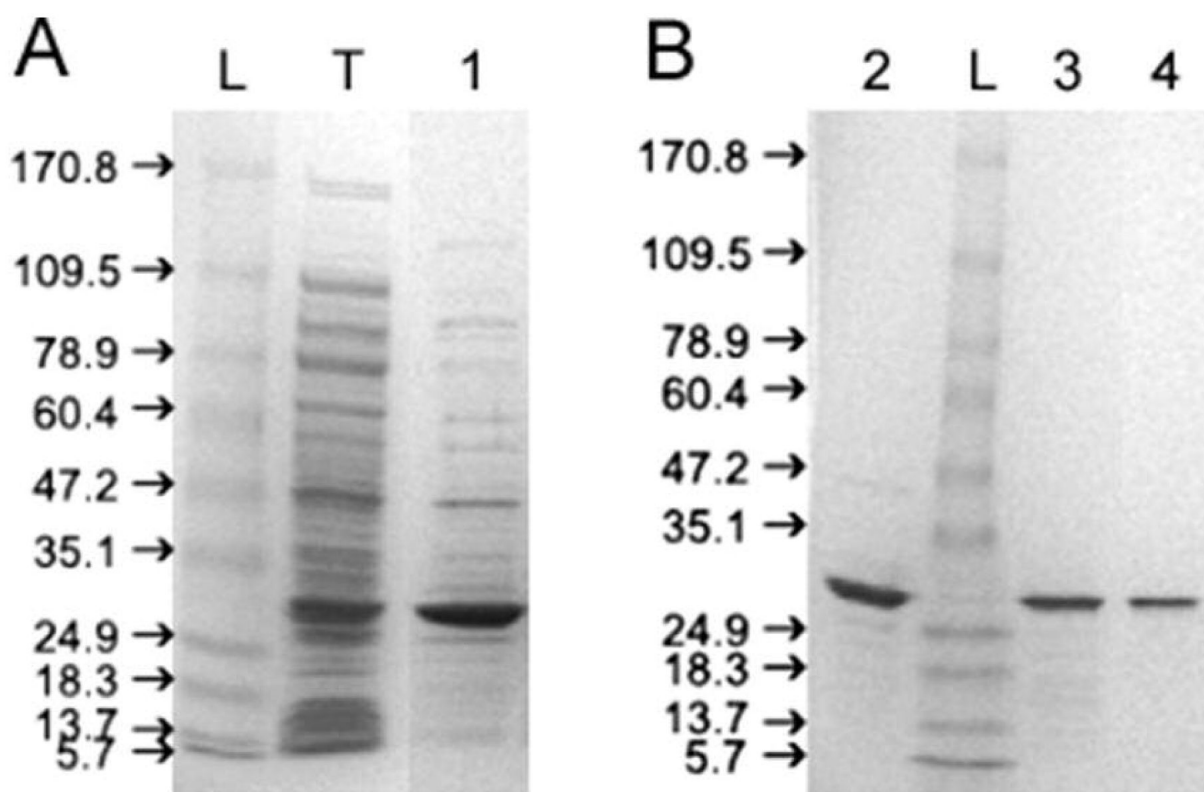


**Figure 1.**

SDS-PAGE showing stepwise purification of mouse  $\beta$ B1-crystallin: L- protein ladder; (A) T- total lysate of bacteria expressing  $\beta$ B1-crystallin; 1- sample after cation exchange; (B) 2- sample after size-exclusion chromatography; 3- sample after partial unfolding by urea and subsequent refolding by dialysis; 4- sample after second size-exclusion chromatography. A discrete band at 28 kDa is seen with a final purity of >95% (Figure 1B, lane 4).

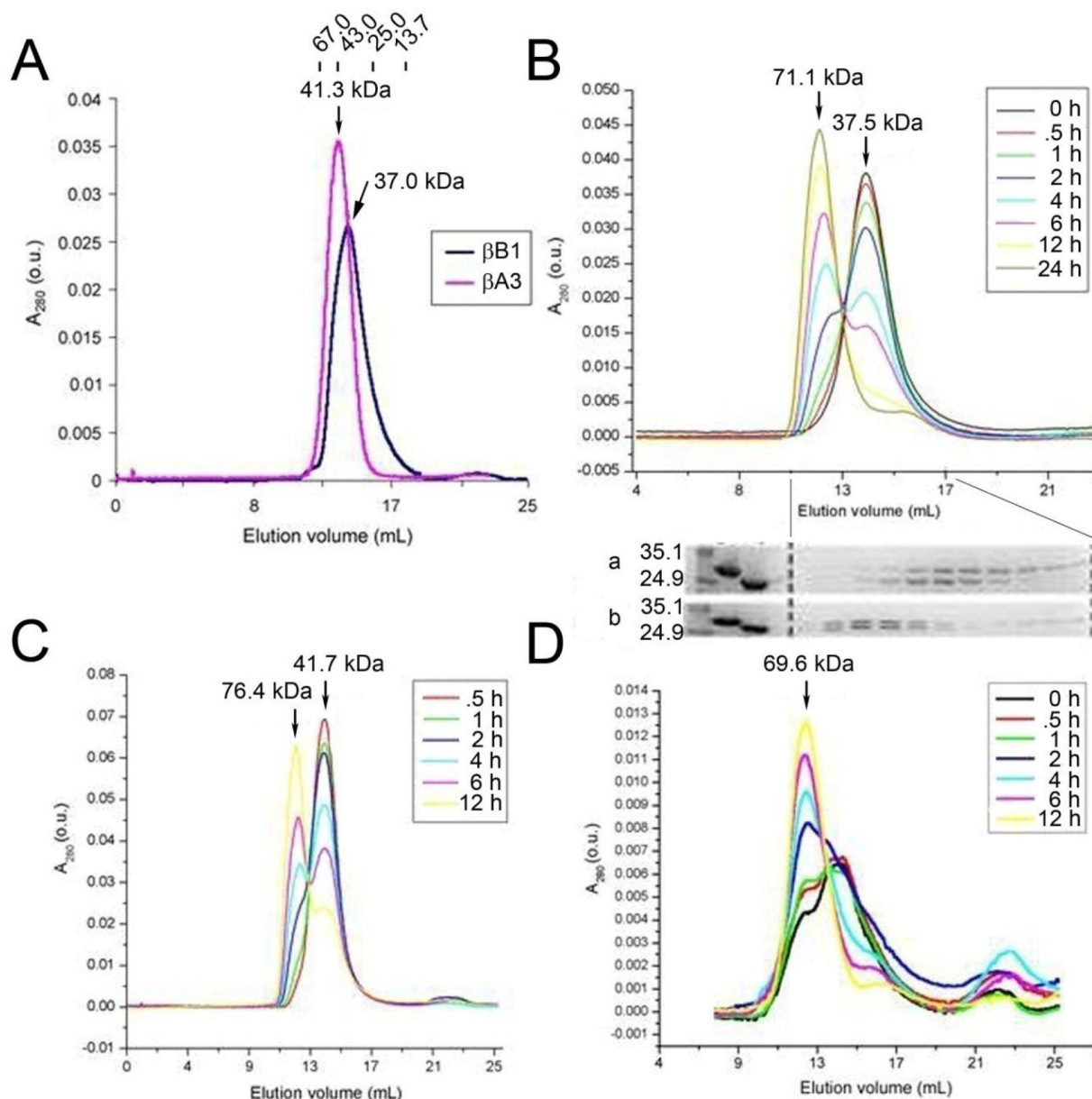


**Figure 2.**

Size-exclusion chromatography of mouse  $\beta$ B1-crystallin and human  $\beta$ A3-crystallins. **Panel A.** Size-exclusion chromatography of mouse  $\beta$ B1-crystallin and human  $\beta$ A3-crystallin, each at 1 mg/mL. The elution points of molecular weight standards (albumin 67.0 kDa, ovalbumin 43.0 kDa, chymotrypsinogen 25.0 kDa, and ribonuclease A 13.7 kDa) are shown at the top for reference. Molecular weights of  $\beta$ B1- and  $\beta$ A3-crystallins were calculated to be 37.0 kDa and 41.3 kDa, respectively. **Panel B.** Size-exclusion chromatography of  $\beta$ B1- and  $\beta$ A3-crystallins mixed at 1 mg/mL. Protein concentration was monitored by absorbance at 280 nm. Chromatograms obtained for each time point after initial mixing of the two crystallins are overlaid to show the trend. Molecular weights of the two peaks at different time points are calculated from the standard curve of the sizing column and averaged to be 71.1 kDa and 37.5 kDa, respectively. A stepwise increase in the higher-molecular-weight species (71.1 kDa) and

a stepwise decrease in the lower-molecular-weight species (37.5 kDa) were observed. SDS-PAGE of the fractions from chromatography runs (a) 0 hr and (b) 24 hr are aligned on the bottom to show contents of the peaks. The first lane refers to protein markers (35.1 and 24.9 kDa). The second and third lanes refer to  $\beta$ B1- and  $\beta$ A3-crystallin standards, respectively. **Panels C and D.** Size-exclusion chromatography of  $\beta$ B1- and  $\beta$ A3-crystallins mixed at (C) 2 mg/mL and (D) 0.5 mg/mL. Averaged molecular weight of each peak is indicated, except for the lower-molecular-weight species in (D), which is indistinct. The small peak observed at the end of each run corresponds to a molecular mass that is lower than the column volume, and is therefore not analyzed.



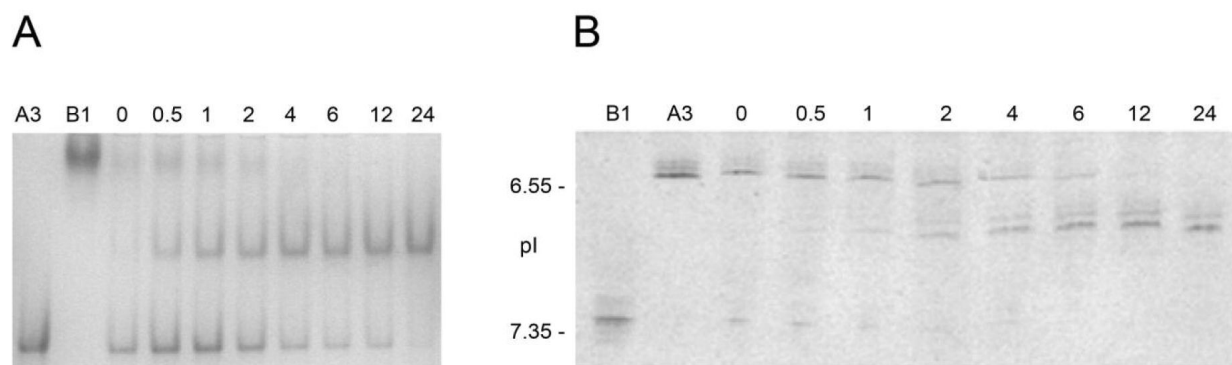


**Figure 3.**

Native gel electrophoresis and isoelectric focusing of  $\beta$ B1- and  $\beta$ A3-crystallins. **Panel A.** Native gel electrophoresis of  $\beta$ B1- and  $\beta$ A3-crystallins mixed at 1 mg/mL each. The black arrow shows the major association product increasing towards end of the incubation. B1:  $\beta$ B1-crystallin only; A3:  $\beta$ A3-crystallin only; 0-24: aliquots taken at corresponding time points (in hours) after initial mixing of the two crystallins. **Panel B.** Isoelectric focusing of mixture of  $\beta$ B1- and  $\beta$ A3-crystallins at 1 mg/mL. Location of two pI markers, human carbonic anhydrase B (pI 6.55) and horse myoglobin-basic band (pI 7.35), are indicated on the left. B1:  $\beta$ B1-crystallin; A3:  $\beta$ A3-crystallin; 0-24: aliquots taken at corresponding time points (in hours) after mixing.

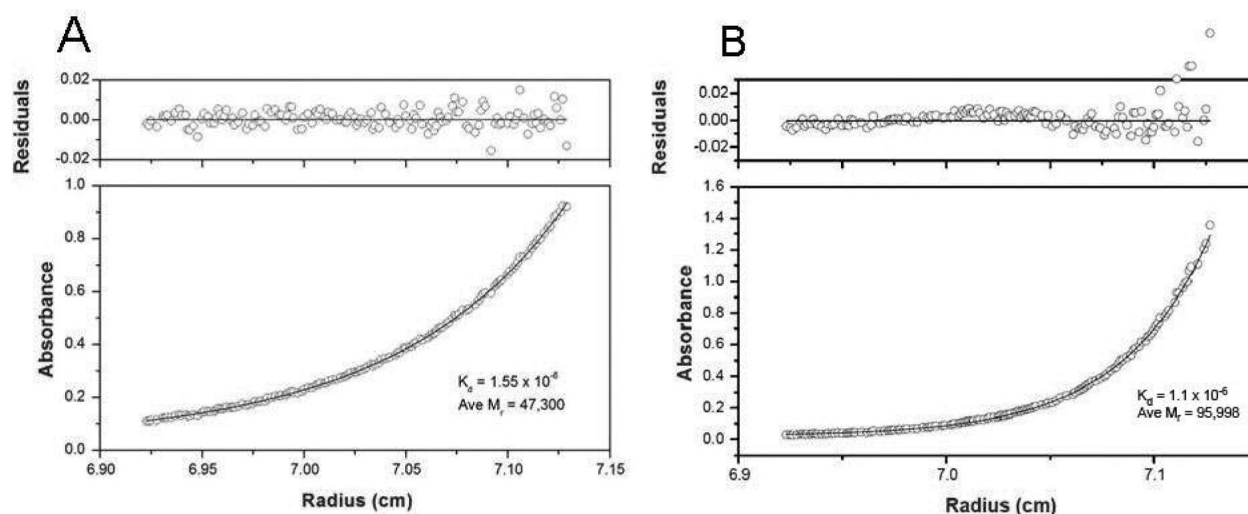


**Figure 4.**

Sedimentation equilibrium of purified mouse  $\beta$ B1-crystallin and of the mouse  $\beta$ B1- and human  $\beta$ A3-crystallin complex are shown. **Panel A.** Sedimentation equilibrium of purified mouse  $\beta$ B1-crystallin at 0.6 mg/mL and 20°C. The absorbance (280 nm) gradient in the ultracentrifuge cell after attaining sedimentation equilibrium is shown in the bottom panel. The solid line indicates the predicted monomer-dimer association model, and the open circles represent the experimental values. The top panel shows the difference between the predicted and the experimental values as a function of radial position (residuals). **Panel B.** Sedimentation equilibrium of the mouse  $\beta$ B1- and human  $\beta$ A3-crystallin complex at 0.6 mg/mL at 20°C. The solid lines indicate the predicted heterodimer-heterotetramer association model, and the open circles represent the experimental values.

**Table 1**

Starting concentrations of  $\beta$ B1- and  $\beta$ A3-crystallins for association experiments.

Starting concentration of each protein in mg/mL ( $\mu$ mol/L)	A <sub>280</sub> of $\beta$ B1-crystallin, o.u.*	A <sub>280</sub> of $\beta$ A3-crystallin, o.u.
0.5 (18)	0.54	0.48
1 (36)	1.14	1.04
2 (72)	2.09	1.85

\* o.u. = Arbitrary optical units

**Table 2**

Comparison of homodimer dissociation constants ( $K_d$ ) and average molecular weight ( $M_r$ ) of mouse  $\beta$ B1-,  $\beta$ A3-, and  $\beta$ B2-crystallins determined by sedimentation equilibrium at 20°C.

Protein	$K_d$ , $\mu$ M	Average $M_r$ , kDa	Predicted $M_r$ of dimer, kDa
$\beta$ B1	1.55	47	56
$\beta$ A3 <sup>*</sup>	0.8	47	50
$\beta$ B2 <sup>*</sup>	5.0	39	46

<sup>\*</sup> Values previously determined (13).